Bentonite-derived materials preferably with nanocarbon incorporation exhibiting exceptionally high dielectric loss at relatively low electrical conductivity

Ailipati Delixiati & D. D. L. Chung

Journal of Materials Science
Full Set - Includes `Journal of Materials Science Letters'

ISSN 0022-2461
Volume 51
Number 2

J Mater Sci (2016) 51:969-978
DOI 10.1007/s10853-015-9426-x

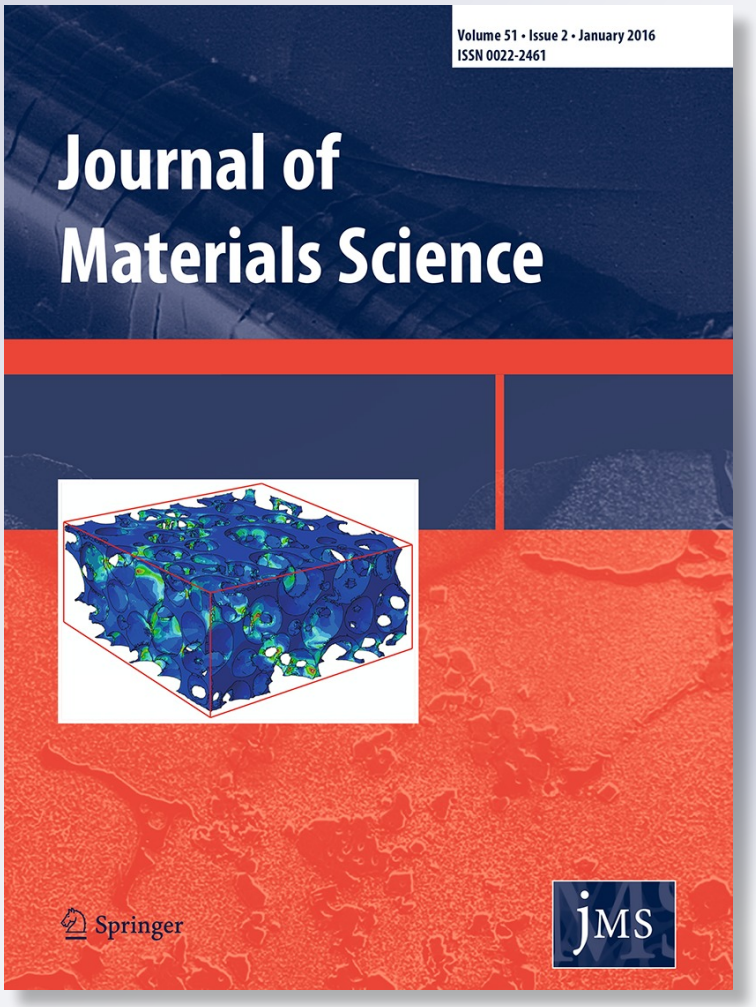

Springer

J Mater Sci (2016) 51:969–978
DOI 10.1007/s10853-015-9426-x

Bentonite-derived materials preferably with nanocarbon incorporation exhibiting exceptionally high dielectric loss at relatively low electrical conductivity

Ailipati Delixiati[1] · D. D. L. Chung[1]

Received: 18 June 2015 / Accepted: 8 September 2015 / Published online: 15 September 2015

Abstract Bentonite-derived monolithic materials with and without distributed nanoscale turbostratic carbon, obtained by hot-pressing organobentonite and bentonite particles, respectively, in the absence of an added binder, exhibit exceptionally high dielectric loss while the electrical conductivity is relatively low. The combination of high dielectric loss and relatively low conductivity has not been previously achieved. An additional advantage of these materials is their high-temperature ability. An application relates to electromagnetic absorption in electronic warfare. Both materials comprise mullite, cristobalite, and disordered clay. The organobentonite-derived material also contains carbon due to organic pyrolysis and exhibits loss angle δ 84.04°–89.52°, the real part of the relative dielectric constant 7.2–25 and conductivity 7.7×10^{-5} to 1.7×10^{-8} S/cm over the frequency range from 10 Hz to 2 MHz (relevant to military communication with submarines and to beacons for aircraft and marine navigation); with increasing frequency, δ decreases, the real and imaginary parts of the relative dielectric constant decrease, and the conductivity increases, all without peaks in the frequency dependence. For the material derived from bentonite, δ is high only above 1400 Hz. The carbon reduces the dielectric connectivity but enhances the conduction connectivity, with the effects decreasing with increasing frequency; it causes the real part of the relative dielectric constant to decrease below 200 Hz, and the absolute value of the imaginary part, conductivity, and δ to increase below ~ 1600 Hz and decrease above ~ 1600 Hz.

Introduction

The interaction of a material with electromagnetic radiation can involve absorption and reflection. It can be exploited to block or divert the radiation. Radiation at frequencies below 50 kHz is used for military communication with submarines. Radiation at frequencies from 150 to 519 kHz (in the long wave band) is used to provide beacons for aircraft and marine navigation through the continuous transmission of the call letters. Radiation at frequencies from 520 to 1720 kHz is used for AM broadcasting. Radiation at frequencies from 87.5 to 108 MHz is used for FM broadcasting. Radiation at frequencies from 3 MHz to 110 GHz is relevant to radar operation, electromagnetic interference (EMI), and low observability (Stealth). The blocking of communication (as in radio jamming) is commonly used in electronic warfare, which refers to the use of the electromagnetic spectrum to attack an enemy or impede enemy assaults. Electronic warfare is directed at denying the opponent the advantage of the electromagnetic spectrum, and ensuring friendly unimpeded access to the spectrum.[1]

This paper focuses on radiation at frequencies from 10 Hz to 2 MHz (2000 kHz). In other words, it covers the following radio frequency bands: 3–30 Hz (extremely low frequency), 30–300 Hz (super low frequency),

✉ D. D. L. Chung
ddlchung@buffalo.edu;
http://alum.mit.edu/www/ddlchung

[1] Composite Materials Research Laboratory, University at Buffalo, State University of New York, Buffalo, NY 14260-4400, USA

[1] Headquarters, Department of the Army (2015) Electronic Warfare in Operations, http://usacac.army.mil/cac2/Repository/FM336/FM336.pdf. Assessed June 13, 2015.

300–3000 Hz (ultra low frequency), 3–30 kHz (very low frequency), 30–300 kHz (low frequency), and 300 kHz–3 MHz (medium frequency). Thus, the frequency range of this work is not relevant to radar operation, electromagnetic interference (EMI), or low observability (Stealth). The frequency range of this study is also chosen because of the feasibility of direct measurement of the relative dielectric constant (related to the capacitance) and conductivity (related to the resistance) using an RLC meter.

Dielectric energy loss and magnetic energy loss are the main mechanisms for the absorption of electromagnetic radiation, with the former being relevant to the electric field component of the radiation and the latter being relevant to the magnetic field component of the radiation. Dielectric loss is provided by dielectric materials, whereas magnetic energy loss is provided by magnetic materials. This paper is focused on the dielectric loss.

The dielectric behavior of a material pertains to the alternating-current (AC) electrical behavior, which includes the electric polarization behavior (as expressed by the real part of the relative dielectric constant, i.e., the real part of the relative permittivity) and the electrical conductivity (which relates to the imaginary part of the relative dielectric constant). The polarization behavior involves the electric dipoles in the material, with the origins of the dipoles including polar molecules, polar functional groups, the asymmetric positioning of the positive and negative ions, and the skewing of the electron clouds. The conductivity involves the movement of charge particles such as electrons and ions in response to the applied electric field.

In the phasor diagram corresponding to the complex plane of the complex relative dielectric constant, the phase angle (loss angle) δ is the angle between the real part and the phasor. The dielectric loss (loss tangent, or tan δ) is given by the ratio of the imaginary part to the real part of the relative dielectric constant. A low-loss material has small values of δ, i.e., δ as low as zero (having a combination of a high value of the real part of the relative dielectric constant and a low value of the imaginary part of the relative dielectric constant). A material with $\delta = 0°$ is said to be a perfect dielectric, which is attractive for low-loss dielectric capacitors. A high-loss material has large values of δ, i.e., δ as high as 90° (having a combination of a low value of the real part of the relative dielectric constant and a high value of the imaginary part of the relative dielectric constant). A material with $\delta = 90°$ is said to be a perfect conductor, which is attractive for AC conduction and electromagnetic absorption.

The imaginary part $-\kappa''$ (where κ'' is negative) of the relative dielectric constant is related to the conductivity σ by the equation

$$-\kappa'' = \sigma/(2\pi\upsilon\varepsilon_o), \tag{1}$$

where υ is the AC frequency and ε_o is the permittivity of free space. The dielectric loss (tan δ) is obtained by using the equation

$$tan\,\delta = -\kappa''/\kappa' = \sigma/(2\pi\upsilon\varepsilon_o\kappa'), \tag{2}$$

where κ' is the real part of the relative dielectric constant of the carbon.

As indicated by Eq. (2), if the real part of the relative dielectric constant is sufficiently small, the electrical conductivity is not necessarily high for a nearly perfect conductor. A relatively low conductivity is attractive for reducing electromagnetic reflection, which promotes electromagnetic detectability. In a battlefield, it is desirable for a warfare material to be not detectable. Furthermore, the conductivity may cause eddy current (induced by the magnetic field in the electromagnetic radiation) and the consequent Joule heating, which can be an issue in temperature-sensitive situations. In addition, the conductivity complicates the packaging, as it may cause the need for an electrically insulating overlayer.

Materials with high values of the real part of the relative dielectric constant (such as ferroelectric materials) cannot provide high δ at a relatively low conductivity. For example, a 600-nm thin film of barium titanate exhibits high real part of the relative dielectric constant up to 1900 and low tan δ up to 0.04 [1]. Even bismuth ferrite ($BiFeO_3$), which is multiferroic, exhibits tan δ equal to only 0.37 [2]. On the other hand, polymers exhibit relatively low values of both the real part of the relative dielectric constant and the conductivity, so that δ cannot be high. Compared to polymers, conventional ceramics (such as alumina) tend to exhibit slightly higher values of the real part of the relative dielectric constant and the conductivity, but both values are still too low for δ to be high. Semimetals such as graphite and semiconductors such as silicon can give high δ due to their high conductivity. Therefore, the attainment of high dielectric loss and relatively low conductivity in the same material has not been previously achieved.

For a given material, the real and imaginary parts of the relative dielectric constant and tan δ all tend to vary with the frequency. Peaks in the plot of tan δ versus frequency are commonly observed and are typically due to ionic and dipolar relaxation, and atomic and electronic resonances at high photon energies above 10 GHz. Although the value of tan δ may be quite high at a peak, the peaks do not provide a high value of tan δ over a wide frequency range. For example, for CdS/α-Fe_2O_3 heterostructures, tan δ equals 0.18 at 7.2 GHz and is only around 0.01 over a broad range of frequencies [3].

Electromagnetic absorption materials that are able to withstand high temperatures are needed for electronic warfare, due to the high temperatures in regions of a battlefield. Carbons are among materials that are effective for absorption, but they are limited in their ability to withstand high temperatures in the presence of oxygen.

Motivated by the above-mentioned technological needs in relation to electronic warfare, this paper is aimed at providing relatively low-conductivity high-temperature materials that exhibit high dielectric loss. The motivation is also scientific, due to the above-mentioned absence of existing materials that exhibit both high dielectric loss and relatively low conductivity. The approach of this work is to achieve the necessary balance between the real part of the relative dielectric constant and the conductivity, so that high δ is achieved at relatively low conductivity.

The most inexpensive and abundant type of ceramic material is minerals in the form of clay. Clay is most commonly in the form of layered silicates. The layers are regularly spaced, with the spacing known as the basal spacing d_{001}.

Bentonite is a form of clay [4, 5]. It consists primarily of crystalline clay minerals that belong to the smectite group. This group includes dioctahedral smectites, such as montmorillonite, which is a 2:1 clay (i.e., each layer consisting of two tetrahedral sheets sandwiching a central octahedral sheet). The basal spacing is 12–13 Å for a single water layer between the clay layers and is 15–16 Å for two water layers between the clay layers [6]. Montmorillonite has more than 50 % octahedral charge. The cation exchange capacity (CEC) [7] refers to the number of positive charges (the number of positive ions multiplied by the charge per ion) that can be held by unit mass of the material. The CEC of montmorillonite is due to the isomorphous substitution of Al^{3+} by Mg^{2+} in the gibbsitic plane (the neutral aluminum hydroxide sheets sandwiched between the silicate sheets). This substitution results in a net negative charge in each of the clay layers. Due to the negative charge, electrostatic interaction causes positive ions (known as counterions, such as Na^{+}, Ca^{2+}, and other ions that may be present) to enter the space between the layers. Sodium bentonite [8] refers to bentonite with Na^{+} ions between the layers. Sodium bentonite and calcium bentonite are two most common types of bentonite. Multiple types of ion can coexist between the layers. Bentonite absorbs water, so that it becomes a hydrate, e.g., hydrated sodium calcium aluminum magnesium silicate hydroxide, with chemical formula $(Na,Ca)_{0.33}(Al,Mg)_2(Si_4O_{10})(OH)_2{\cdot}nH_2O$. Montmorillonite particles are white, plate-shaped, with an average diameter of about 1 μm and a monoclinic crystal structure. The dielectric behavior of bentonite in the presence of either water or a salt solution has been previously reported [6, 9].

This paper is aimed at providing a nearly perfect conductor (with δ approaching 90° over a substantial range of frequency) that has a relatively low conductivity and can withstand high temperatures (say, 1000 °C). This combination of properties is found in this work to be exhibited by bentonite-derived materials, namely materials obtained by hot pressing (in the absence of a binder) either bentonite or organobentonite [10]. In this paper, "bentonite" refers to the material without the organic component. Prior to the hot pressing, the bentonite or organobentonite is in particle form. However, after the hot pressing at 1000 °C and 21 MPa, the material becomes a coherent monolithic sheet that exhibits high modulus, high strength, low porosity, and high temperature resistance, with phases including mullite, cristobalite, and disordered clay [10].

Through the hot pressing, the organic component of the organobentonite (in the form of particles) is converted to nanoscale turbostratic carbon, thus resulting in a monolithic ceramic-carbon hybrid with ceramics being the majority and carbon being the minority [10]. Raman scattering, X-ray diffraction, and other results are in Ref. 10 to support the above statement. Both the organic and inorganic parts of the organobentonite serve as binders [10]. The hybrid exhibits flexural strength 180 MPa and modulus 69 GPa, but the ductility is low [10]. It also functions as a reinforcing filler and a binder for carbon/carbon (C/C) composites [10].

Although the DC electrical conductivity of hot-pressed bentonite/organobentonite has been previously reported [10], the AC conductivity and the relative dielectric constant (real or imaginary part) have not been previously reported. This paper provides AC measurement of both the conductivity and the relative dielectric constant (real and imaginary parts) over a substantial frequency range. The AC behavior pertains to both the conduction behavior and the dielectric behavior, whereas the DC behavior pertains to the conduction behavior only.

Experimental methods

Materials

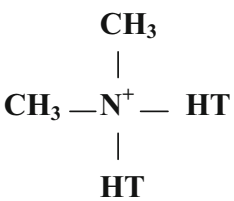

The organobentonite used is montmorillonite that has been intercalated with a dimethyl hydrogenated tallow

ammonium. The hydrogenated tallow (abbreviated HT in the schematic above) involves ~65 % fatty acids with 18 carbon atoms in the alkyl carbon chain, ~30 % fatty acids with 16 carbon atoms in the chain, and ~5 % fatty acids with 14 carbon atoms in the chain. The cation exchange capacity is 125 cmol/kg. The density is 1.66 g/cm^3. The loss on ignition is 43 wt%. The particles are white, with size such that 10 % is less than 2 μm, 50 % is less than 6 μm, and 90 % is less than 13 μm. Each layer is 1-nm thick and 70–150 nm across, with an aspect ratio 70–150. If it were exfoliated, the specific surface area would exceed 750 m^2/g. The basal spacing $d_{001} = 31.5$ Å [10]. This organobentonite is the product designated Cloisite 15, as provided by Rockwood, Inc., Gonzales, TX. Cloisite 15 is the current version of Cloisite 15A [10], which has been discontinued by the manufacturer.

The bentonite (without an organic component) is sodium bentonite (Asbury Graphite Mills, Inc., Asbury, NJ, M325). It contains 2–6 wt% free SiO_2 and has less than 10 wt% moisture. It has particle size 44 μm, cation exchange capacity (CEC) 92 cmol/kg, true density 2.3 g/cm^3, and negligible solubility in water.

Hot-pressing method

Bentonite/organobentonite particles are subjected to hot pressing using the method of Wang et al. [10]. Indirect resistance heating is conducted using a graphite mold that consists of a cylindrical mold cavity (inside diameter 32.92 mm and outside diameter 76.37 mm) and a matched cylindrical graphite piston (diameter 31.75 mm).

The hot-pressed bentonite is in the form of a disk of diameter 31.0 ± 0.1 mm. It is obtained by hot-pressing bentonite powder in the amount of 4.000 ± 0.001, 5.000 ± 0.001, or 6.000 ± 0.001 g, so as to obtain a hot-pressed specimen of thickness 1.69 ± 0.05 mm, 2.29 ± 0.06 mm, or 2.56 ± 0.04 mm, respectively, and density 2.465 ± 0.034, 2.466 ± 0.019, or 2.466 ± 0.017 g/cm^3, respectively.

The hot-pressed organobentonite is also in the form of a disk of diameter 31.0 ± 0.1 mm. It is obtained by hot-pressing organobentonite powder in the amount of 6.000 ± 0.001, 7.000 ± 0.001, or 8.000 ± 0.001 g, so as to obtain a hot-pressed specimen of thicknesses 1.80 ± 0.02 mm, 2.04 ± 0.02 mm, or 2.39 ± 0.002 mm, respectively, and densities 2.366 ± 0.002, 2.365 ± 0.026, or 2.360 ± 0.002 g/cm^3, respectively.

Bentonite/organobentonite particles in three different amounts (as mentioned above) are separately put into the mold cavity, such that the particles are sandwiched by exfoliated graphite particles [11], which are used to facilitate demolding after hot pressing. During hot pressing, the exfoliated graphite is compressed, thereby forming a sheet known as "flexible graphite," which is a high-temperature gasket material [12]. The flexible graphite sheet is formed in the absence of a binder, due to the mechanical interlocking among the pieces of exfoliated graphite, which has a cellular structure. Hot pressing is conducted under nitrogen at a flow of 70 ml/min. The temperature is first raised from room temperature (~20 °C) to 300 °C in a period of 1.0 h without pressure application, with the heating rate being constant. After this, the temperature is increased from 300 to 700 °C over a period of 1.0 h at a uniaxial pressure of 21.00 ± 0.25 MPa, again with the heating rate being constant. Then the temperature is increased from 700 to 1000 °C over a period of 1.0 h at the same pressure of 21.00 ± 0.25 MPa, again with the heating rate being constant. Finally, the temperature is maintained at 1000 °C for 30 min at the same pressure of 21.00 ± 0.25 MPa. After this, the hot-pressed material is furnace cooled under nitrogen, till the temperature has decreased to around 300 °C. At this point, the nitrogen purging is stopped.

Method of measuring the real part of the relative dielectric constant

A precision RLC meter (Quadtech 7600) is used to measure the real part of the relative dielectric constant in the frequency range from 10 Hz to 2 MHz. The parallel RC circuit model is used. The electric field is applied between two copper foils (each of thickness 62 μm) that sandwich the specimen. The copper foil and a steel weight above the foil provide a pressure of 4.3 kPa (0.63 psi) during testing for the purpose of improving the electrical contact between the copper foil and the specimen. To minimize the current when the real part of the relative dielectric constant is measured, a glass-fiber-fabric reinforced Teflon film (CS Hyde Company, Lake Villa, IL) of thickness 75 μm, with the real part of the relative dielectric constant being equal to 2.34 (as measured at 1.000 kHz), is used to insulate the specimen from each of the two copper foils. The Teflon film is circular of diameter 31.0 mm (area 754 mm^2). The specimen is in the form of a solid disk of this same diameter.

Both the volume of the specimen and the interface between the specimen and each of the two copper foils contribute to the measured capacitance. In order to decouple the volumetric and interfacial contributions to the measured capacitance, each type of material is tested at three different thicknesses.

As shown by the equivalent circuit in Fig. 1, the measured capacitance C is that of the series combination of the specimen capacitance $l/(\varepsilon_0 \kappa A)$ and each of the two specimen–copper interface capacitances (each being C_i), where ε_0 is the permittivity of free space (8.85×10^{-12} F/m), κ is

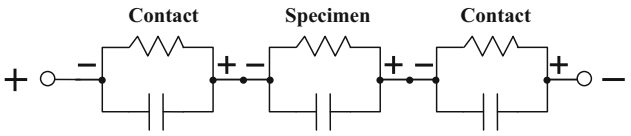

Fig. 1 Equivalent circuit model for a specimen that is electrically in series with two contacts. Each circuit element is modeled as a resistor and a capacitor in parallel. The contact refers to the interface between the specimen and an electrical contact

the real part of the relative dielectric constant of the specimen, A is the contact area, which is the same as the specimen area, and l is the thickness of the specimen. Based on the Rule of Mixtures for capacitances in series,

$$1/C = 2/C_i + l/(\varepsilon_0 \kappa A). \quad (3)$$

The plot of $1/C$ versus l is a straight line with the intercept equal to $2/C_i$ at the $1/C$ axis (at $l = 0$) and the slope equal to $1/(\varepsilon_0 \kappa A)$. From the slope, κ is obtained.

Hot-pressed bentonite/organobentonite specimens, with each type of material at three different thicknesses described in "Hot pressing method" section, are tested. Though the thickness of the specimen varies, the electric field is fixed at 0.65 V/mm by adjustment of the AC voltage (in the range from 0.27 to 1.66 V).

Method of measuring the electrical resistivity

The AC resistance is measured in the same frequency range and in the same way as the capacitance ("Method of measuring the real part of the relative dielectric constant" section), except that the two Teflon films are absent, so that the specimen is in direct contact with the copper contact. The measured resistance is a series combination of the volume resistance and two interfacial resistances. The equivalent circuit is shown in Fig. 1. The AC resistance is measured by using the QuadTech Model 7200 Precision RLC meter operated with the parallel RC configuration (as for the measurement of the real part of the relative dielectric constant).

Resistivity measurement is also conducted by using silver paint (in conjunction with aluminum foil in the absence of an applied pressure during testing) as the electrical contact material. This is in contrast to the use of pressure contacts, as described above. The results obtained by using silver paint are found to be consistent with those obtained by using pressure contacts.

Unlike the interfacial resistivity, which is an area-independent interface property, the volume electrical resistivity is a volumetric geometry-independent material property. In order to decouple the volumetric and interfacial contributions to the measured resistance, three thicknesses of each material are involved in the testing.

The measured resistance R between the two copper contacts that sandwich the specimen in the form of a solid plate is the series combination of the volume resistance R_s of the specimen and the resistance R_i of each of the two interfaces between the specimen and a copper contact (Fig. 1), i.e.,

$$R = R_s + 2R_i. \quad (4)$$

By measuring R at three specimen thicknesses, the curve of R versus thickness is obtained. The intercept of this curve with the vertical axis at $l = 0$ equals $2R_i$, whereas the slope of this curve equals R_s/l, where R_s is the specimen resistance for the specimen of thickness l. The specimen resistivity is obtained by multiplying R_s/l by the specimen area A. The volumetric resistivity ρ_s of the specimen is then given by

$$\rho_s = R_s A/l. \quad (5)$$

Thermogravimetric analysis method

Thermogravimetric analysis (TGA) is conducted to observe the weight loss upon heating so as to evaluate the ability to withstand high temperatures. It involves measuring the weight of a specimen during heating at a controlled heating rate in the presence of purging nitrogen gas. The instrument is TGA 7 of Perkin-Elmer Corp. The heating rate is 5 °C/min from 25 to 900 °C. Immediately after reaching the maximum temperature of 900 °C, furnace cooling is conducted at an approximate cooling rate of 20 °C/min.

Results and discussion

Thermogravimetric analysis

Figure 2 shows that hot-pressed organobentonite/bentonite exhibits very little weight loss up to the maximum test

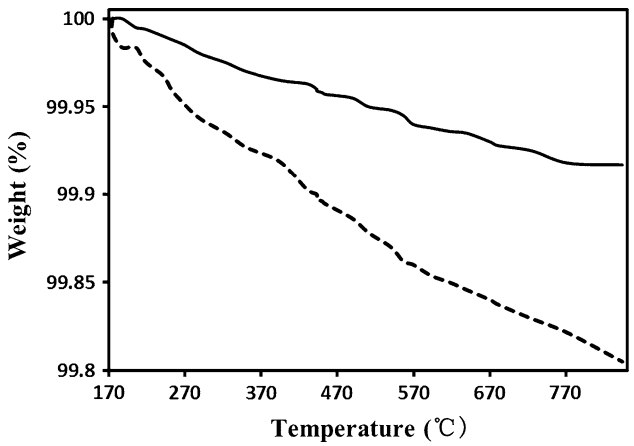

Fig. 2 Thermogravimetric results during heating of hot-pressed organobentonite (*upper curve*) and hot-pressed bentonite (*lower curve*)

temperature of about 800 °C. The maximum fractional weight loss is 0.08 and 0.18 % for hot-pressed organobentonite and hot-pressed bentonite, respectively. This means that hot-pressed organobentonite is superior to hot-pressed bentonite in the ability to withstand high temperatures. This finding is consistent with that previously reported [10]. In spite of the presence of carbon, hot-pressed organobentonite is more oxidation resistant than hot-pressed bentonite. This is probably due to the lower porosity (not measured) that results from the contribution of carbon to the binding action in hot-pressed organobentonite. A lower porosity for the hot-pressed organobentonite is suggested by the higher flexural strength compared to hot-pressed bentonite [10]. Since the hot pressing is conducted at 1000 °C, both materials are able to withstand at least 1000 °C.

AC electrical behavior of hot-pressed organobentonite

Figure 3 shows the plot of $1/C$ versus thickness and the plot of the resistance versus thickness for hot-pressed organobentonite. The plots are linear, supporting the validity of the method. The slope of the plot of $1/C$ versus thickness relates to the real part of the relative dielectric constant. The slope of the plot of resistance versus thickness gives the resistivity.

As shown in Fig. 4a, b, the real and imaginary parts (absolute values) of the relative dielectric constant and the loss angle δ decrease with increasing frequency, while the conductivity increases with increasing frequency. The variation of all the above quantities with frequency is essentially monotonic, with the absence of peaks. This indicates the absence of resonance behavior. The decrease of the real part of the relative dielectric constant with frequency is due to the dipolar relaxation. The decrease of the absolute value of the imaginary part of the relative dielectric constant occurs in spite of the increase in conductivity and is due to the inherent trend of this quantity decreasing with increasing frequency. Both the real and imaginary parts (absolute values) of the relative dielectric constant decrease sharply with increasing frequency at low frequencies and level off at high frequencies. The leveling off of the imaginary part of the relative dielectric constant occurs at a higher frequency than the leveling off of the real part of the relative dielectric constant.

The increase of the conductivity with increasing frequency (Fig. 4c) is attributed to the decreasing excursion of the conduction charge carrier (such as electrons) in an AC cycle as the frequency increases and the consequent lower chance of the carriers to encounter scattering sites associated with defects or interfaces. The decrease of δ with increasing frequency (Fig. 4d) occurs in spite of the

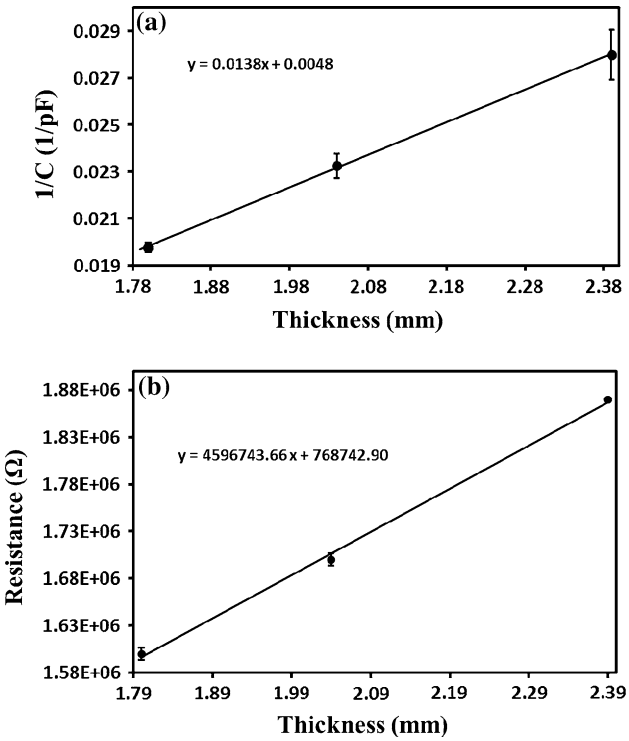

Fig. 3 Plots of the raw capacitance and resistance data of hot-pressed organobentonite at 100 Hz. **a** Plot of $1/C$ versus thickness, with the reciprocal of the slope related to the real part of the relative dielectric constant. **b** Plot of the resistance versus thickness, with the slope related to the resistivity

decrease in the real part of the relative dielectric constant and the increase in conductivity. It is attributed to the inherent tendency for δ to decrease with increasing frequency.

The real part of the relative dielectric constant decreases from 25 at 10 Hz to 7.2 at 2 MHz, with the value being 9.4 at 1 kHz. The absolute value of the imaginary part of the relative dielectric constant decreases from 3000 at 10 Hz to 500 at 100 Hz and to 100 at 4000 Hz, and it essentially levels off above 4000 Hz, with the value being 200 at 1 kHz. The conductivity increases from 1.7×10^{-8} S/cm at 10 Hz to 7.7×10^{-5} S/cm at 2 MHz, with the value being 1.2×10^{-7} S/cm at 1 kHz. The loss angle δ decreases from 89.52° at 10 Hz to 84.04° at 2 MHz, with the value being 87.55° at 1 kHz; this corresponds to tan δ decreasing from 119 to 9.58, with the value being 23.4 at 1 kHz.

The real part of the relative dielectric constant is in the range for silicon, graphite, and diamond [13] and is higher than the value of 6.0 at 1 MHz for mullite [14] and the value of 3.8 for fused silica [15]. The conductivity is low compared to metals and carbons, but is high compared to most ceramics. Among ceramics, mullite exhibits conductivity $<10^{-13}$ S/cm [14] and fused silica exhibits conductivity $<10^{-20}$ S/cm [15]. In spite of the presence of mullite

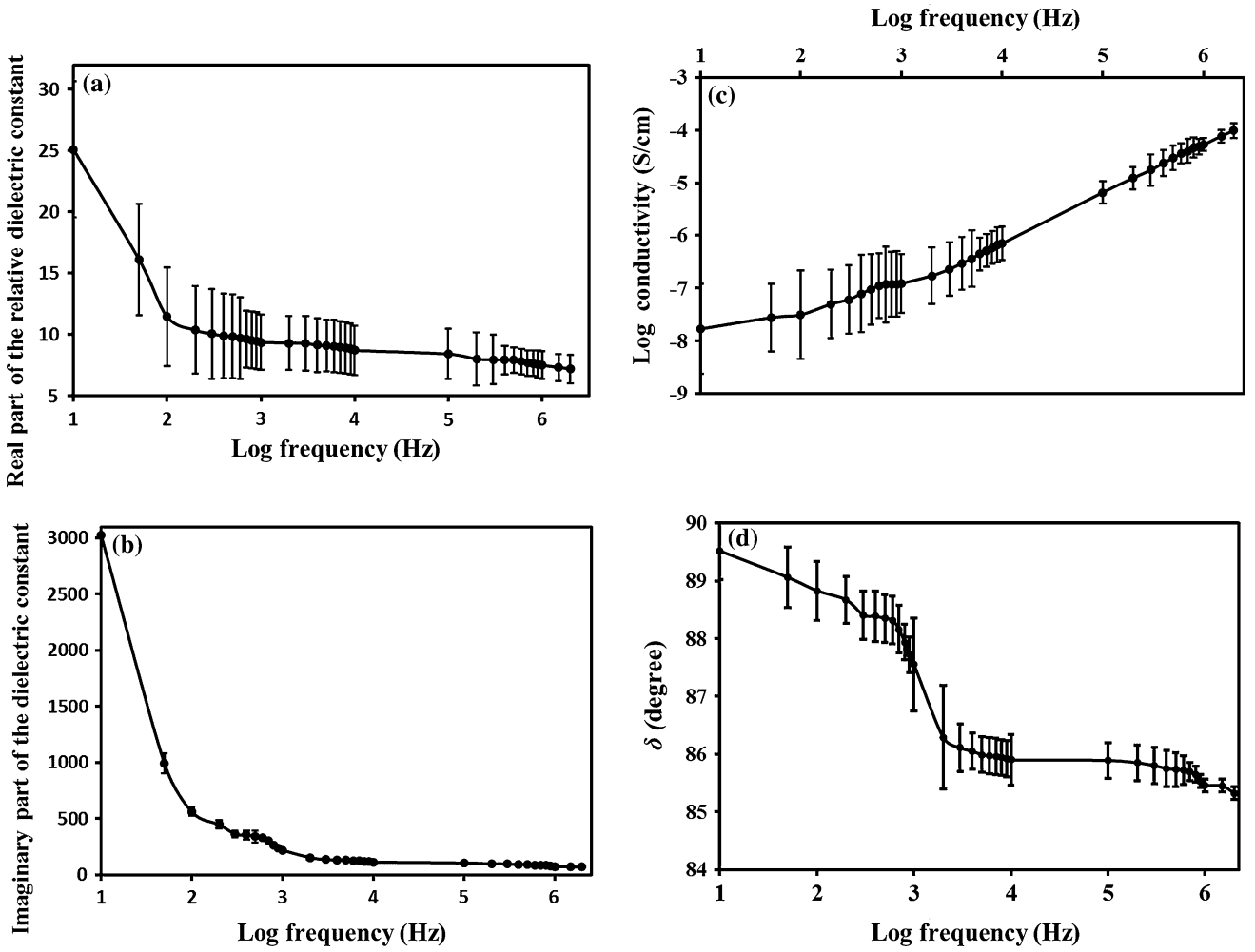

Fig. 4 AC electrical behavior of hot-pressed organobentonite showing the effect of frequency from 10 Hz to 2 MHz. **a** Real part of the relative dielectric constant. **b** The absolute value of the imaginary part of the relative dielectric constant, which is negative. **c** Electrical conductivity (log scale). **d** Loss angle δ

and cristobalite (akin to fused silica) [10], the hot-pressed organobentonite exhibits higher values of both the real part of the relative dielectric constant and the conductivity than mullite or fused silica. This is attributed to the carbon present in the hot-pressed organobentonite. The δ angle remains very high throughout the wide frequency range studied, so that the hot-pressed organobentonite is a nearly perfect conductor throughout the frequency range.

The δ values (84.0°–89.5°, 10 Hz–2 MHz) of the hot-pressed organobentonite are much higher than the value of 11° previously reported at 100 Hz for purified calcium bentonite [16], much higher than the value of 0.11° (1 MHz) for mullite [14], higher than the values in the range from 5.7° to 84.3° previously reported for an exfoliated graphite polymer-matrix composite at 1 kHz–1 MHz (although the value rises sharply below 1 kHz to a maximum at 89.4° at 100 Hz) [17], higher than the value of 39° previously reported for an exfoliated graphite carbon-nanotube polymer-matrix composite at 10 kHz–10 MHz (though the value increases below 10 kHz to a maximum of 86.7° at 100 Hz) [18], higher than the values ranging from 3° to 35° previously reported for an exfoliated graphite epoxy-matrix composite at 50 Hz–1 MHz [19], higher than the value of 24° previously reported for a graphite-nanosheet clay polymer-matrix composite [20], and higher than the value ranging from 14° at 0.1 MHz to 77.5° at 50 Hz previously reported for a graphite particle (10–20 μm particle size) clay-matrix composite (with the clay being kaolinite) [21]. The above comparison with prior work indicates that the hot-pressed organobentonite is superior to the materials of the prior work in providing a high value of δ over a wide frequency range.

The exceptionally high dielectric loss of the hot-pressed organobentonite is attributed to the presence of disordered clay (86 vol%) and turbostratic carbon (14 vol%) and the ceramic-carbon hybrid nanostructure [10]. The graphite

particle clay-matrix composite of prior work [22], as fabricated at 1100 °C, contains graphite (with crystallite size less than 50 nm), cristobalite, and disordered clay. In contrast, the hot-pressed organobentonite of this work contains turbostratic carbon, cristobalite, mullite, and disordered clay [10]. Although the carbon in the clay-matrix composite is graphite [22] and that in the hot-pressed organobentonite is turbostratic carbon [10], the conductivity is only 2×10^{-8} S/cm for the clay-matrix composite in the frequency range in which the conductivity reaches a plateau, whereas it is in the range from 1×10^{-4} to 2×10^{-8} S/cm for the hot-pressed organobentonite. The lower conductivity of the clay-matrix composite is probably due to the lower degree of connectivity of its carbon phase and contributes to causing δ to be relatively low.

Comparison of hot-pressed organobentonite and hot-pressed bentonite in terms of the AC electrical behavior

As shown in Fig. 5a, hot-pressed organobentonite exhibits lower values of the real part of the relative dielectric constant than hot-pressed bentonite at frequencies below 200 Hz, above which the values are essentially equal for the two materials. The higher is the frequency, the less is the difference in the real part of the relative dielectric constant between the two materials. That the values are lower for hot-pressed organobentonite at low frequencies is attributed to the nanoscale-distributed carbon in this material hindering the dielectric connectivity of the ceramic phases. As the frequency increases, the excursion of the polarization charges in a cycle decreases, thereby causing the distributed carbon to have less influence on the polarization.

In contrast to the decrease with increasing frequency for the absolute value of the imaginary part of the relative dielectric constant of hot-pressed organobentonite, this quantity tends to increase with increasing frequency for hot-pressed bentonite (Fig. 5b). This trend for hot-pressed bentonite is attributed to the increase in conductivity with increasing frequency (Fig. 5c). That the trends are opposite for hot-pressed organobentonite and hot-pressed bentonite is because the increase in conductivity with increasing frequency is more significant for the latter. The absolute value of the imaginary part of the relative dielectric constant of hot-pressed bentonite is less than that of hot-pressed organobentonite below 1400 Hz, but is greater than that of hot-pressed organobentonite above 1400 Hz. This means that the presence of carbon in the hot-pressed organobentonite increases the absolute value of the imaginary part of the relative dielectric constant below 1400 Hz, but decreases this quantity above 1400 Hz. A similar cross-over for the two materials occurs for the variation of the conductivity with the frequency (Fig. 5c).

As shown in Fig. 5c, the conductivity is higher for hot-pressed organobentonite than hot-pressed bentonite at frequencies below 1800 Hz, but is lower for hot-pressed organobentonite than hot-pressed bentonite above 1800 Hz. This means that the presence of carbon in the hot-pressed organobentonite increases the conductivity below 1800 Hz, but decreases the conductivity above 1800 Hz. The lower conductivity of hot-pressed bentonite in the low frequency regime is attributed to the relatively large excursion of the conduction charges in a cycle in the low frequency regime and the consequent relatively large positive influence of the distributed carbon on the conductivity. However, in the high frequency regime, the carbon has relatively little influence on the conductivity, while the ceramic part of the hot-pressed organobentonite is probably less conductive than the hot-pressed bentonite (probably due to the difference in ceramic phase proportions [10] and possible differences in the degree of order of the disordered clay and in the microstructure).

As shown in Fig. 5d, δ is higher for hot-pressed organobentonite than hot-pressed bentonite at frequencies below 1600 Hz, but is lower for hot-pressed organobentonite than hot-pressed bentonite above 1600 Hz. This means that the carbon increases δ below 1600 Hz, but decreases δ above 1600 Hz. The higher δ for hot-pressed organobentonite in the low frequency regime is attributed to the higher conductivity (Fig. 5c) and the lower real part of the relative dielectric constant (Fig. 5a). The lower δ for hot-pressed organobentonite in the high frequency regime is attributed to the lower conductivity (Fig. 5c). Hot-pressed bentonite is thus a more perfect conductor than hot-pressed organobentonite in the high frequency regime, but it is a much poorer conductor than hot-pressed organobentonite in the low frequency regime. With both regimes taken into consideration, hot-pressed organobentonite is a more perfect conductor than hot-pressed bentonite.

Conclusion

Bentonite-derived monolithic materials with and without distributed nanoscale turbostratic carbon, obtained by hot-pressing organobentonite and bentonite particles, respectively, at 1000 °C and 21 MPa in the absence of an added binder, exhibit exceptionally high dielectric loss while the electrical conductivity is relatively low. They are potentially attractive for electromagnetic absorption in electronic warfare, even at high temperatures (up to around 1000 °C). Hot-pressed organobentonite is more oxidation resistant than hot-pressed bentonite.

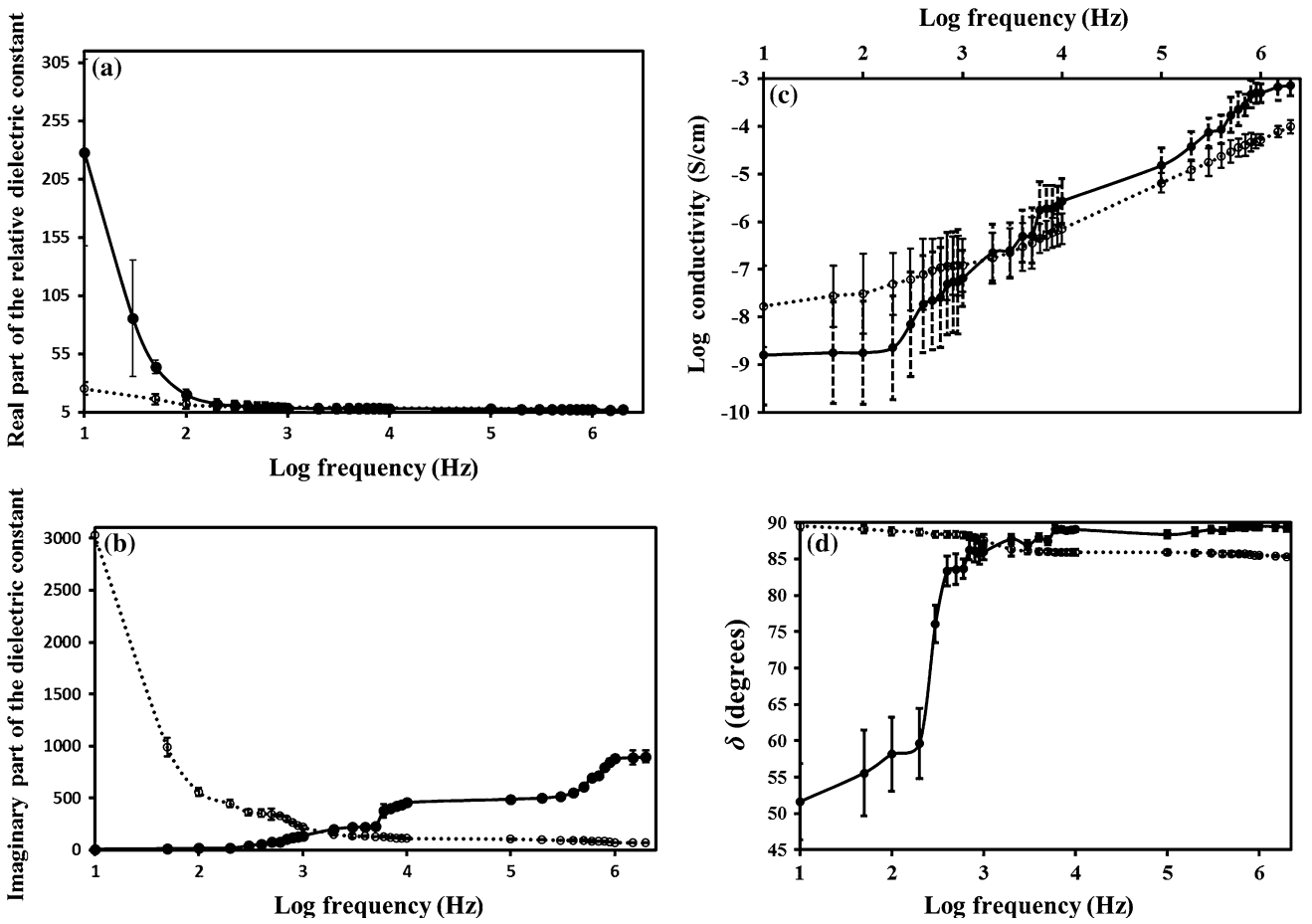

Fig. 5 Comparison of the AC electrical behavior of hot-pressed organobentonite (*open circles*) and hot-pressed bentonite (*solid circles*). **a** Real part of he relative dielectric constant. **b** The absolute value of the imaginary part of the relative dielectric constant, which is negative. **c** Electrical conductivity (log scale). **d** Loss angle δ

Hot-pressing organobentonite gives a previously reported ceramic-carbon nanostructured hybrid [10]. This work shows that this material is a nearly perfect AC conductor in the frequency range from 10 Hz to 2 MHz. The real part of the relative dielectric constant decreases from 25 at 10 Hz to 7.2 at 2 MHz, the absolute value of the imaginary part of the relative dielectric constant decreases from 3000 at 10 Hz to 100 at 2 MHz, the conductivity increases from 1.7×10^{-8} S/cm at 10 Hz to 7.7×10^{-5} S/cm at 2 MHz, and δ decreases from 89.52° at 10 Hz to 84.04° at 2 MHz (corresponding to tan δ decreasing from 119 at 10 Hz to 9.6 at 2 MHz). The variation of all three quantities with frequency is essentially monotonic, with the absence of peaks.

Comparison of hot-pressed organobentonite and hot-pressed bentonite shows that the nanoscale carbon present in the former due to the pyrolysis of the organic component of the organobentonite causes the relative dielectric constant (real part) to decrease below 200 Hz, causes the absolute value of the imaginary part of the relative dielectric constant to increase below 1400 Hz and decrease above 1400 Hz, causes the conductivity to increase below 1800 Hz and decrease above 1800 Hz, and causes δ to increase below 1600 Hz and decrease below 1600 Hz. In other words, the carbon causes the absolute value of the imaginary part of the relative dielectric constant, the conductivity, and δ to all increase below $\sim$1600 Hz and all decrease above $\sim$1600 Hz. Above 200 Hz, the relative dielectric constant (real part) is essentially equal for the two materials. These effects of carbon are attributed to the negative effect of carbon on the dielectric connectivity, the positive effect of carbon on the conduction connectivity, and the decreasing effects of carbon on both types of connectivity as the frequency increases.

Hot-pressed organobentonite gives high δ values that range from 89.5° at 10 Hz to 84.0° at 2 MHz (decreasing with increasing frequency), whereas hot-pressed bentonite gives high values only above 1400 Hz. Hot-pressed organobentonite is a more perfect conductor than hot-pressed bentonite, when both frequency regimes are

considered together. Hot-pressed organobentonite is also superior to the materials of prior work (including a wide range of clay, carbon, and magnetic materials) in providing a high value of δ over a wide frequency range.

References

1. Brennecka GL, Ihlefeld JF, Maria J, Tuttle BA, Clem PG (2010) Processing technologies for high-permittivity thin films in capacitor applications. J Am Ceramic Soc 93:3935–3954
2. Yuana J, Hou Z, Yang H, Li Y, Kang Y, Song W, Jin H, Fang X, Cao M (2013) High dielectric loss and microwave absorption behavior of multiferroic $BiFeO_3$ ceramic. Ceramics Int 39:7241–7246
3. Shi X, Cao M, Yuan J, Zhao Q, Kang Y, Fang X, Chen Y (2008) Nonlinear resonant and high dielectric loss behavior of CdS/α-Fe_2O_3 heterostructure nanocomposites. Appl Phys Lett 93:183118-1–183118-4
4. Novelli G (2003) Bentonite: an industrial mineral at mankind service. Annali di Chimica (Rome, Italy) 93:129–136
5. Uddin F (2008) Clays, nanoclays, and montmorillonite Minerals. Metall Mater Trans A 39A:2804–2814
6. Kaden H, Koeniger F, Stroemme M, Niklasson GA, Emmerich K (2013) Low-frequency dielectric properties of three bentonites at different adsorbed water states. J Colloid Interface Sci 411:16–26
7. Bowen P, Carry C (2002) From powders to sintered pieces: forming, transformations and sintering of nanostructured ceramic oxides. Powder Technol 128:248–255
8. Laird D, Fleming P (2008) Soil Science Society of America Book Series 5(Methods of Soil Analysis, Part 5: Mineralogical Methods), pp 485–508
9. Kaya A (2001) Electrical spectroscopy of kaolin and bentonite slurries. Turk J Eng Environ Sci 25:345–354
10. Wang A, Gao X, Giese RF Jr, Chung DDL (2013) A ceramic-carbon hybrid as a high-temperature structural monolith and reinforcing filler and binder for carbon/carbon composites. Carbon 59:76–92
11. Chen P, Chung DDL (2013) Viscoelastic behavior of the cell wall of exfoliated graphite. Carbonl 61:305–312
12. Chung DDL (2000) Flexible graphite for gasketing, adsorption, electromagnetic interference shielding, vibration damping, electrochemical applications, and stress sensing. J Mater Eng Perf 9(2):161–163
13. Wikipedia (2015) Relative permittivity. http://en.wikipedia.org/wiki/Relative_permittivity. Accessed 1 Nov 2014
14. CoorsTek (2015) Mullite material properties. http://www.coorstek.com/materials/ceramics/mullite.php. Accessed 31 Oct 2014
15. AZO Materials (2000–2015) Silica–silicon dioxide (SiO_2), http://www.azom.com/article.aspx?ArticleID=1114#_Key_Properties. Assessed 31 Oct 2014
16. Kuecuekcelebi H, Durmus H, Deryal A, Taser M, Karakaya N (2012) Activation energy of polarization due to electrical conductivity and dipole rotation in purified Ca-bentonite. Appl Clay Sci 62–63:70–79
17. Gu L, Liang G, Shen Y, Gu A, Yuan L (2014) Preparation of high k expanded graphite/$CaCuTi_4O_{12}$/cyanate ester composites with low dielectric loss through controlling the interfacial action between conductors and ceramic. Compos B 58:66–75
18. Cao L, Zhang W, Zhang X, Yuan L, Liang G, Gu A (2014) Low-cost preparation of high-k expanded graphite/carbon nanotube/cyanate ester composites with low dielectric loss and low percolation threshold. Ind Eng Chem Res 53:2661–2672
19. Xie Y, Yu D, Min C, Guo X, Wan W, Zhang J, Liang H (2009) Expanded graphite-epoxy composites with high dielectric constant. J Appl Polymer Sci 112(6):3613–3619
20. Li Y, Tjong SC (2012) Electrical properties of binary PVDF/clay and ternary graphite-doped PVDF/clay nanocomposites. Curr Nanosci 8(5):732–738
21. Goswami R, Chakravartty SC, Krishna JBM, Bose E, Das D, Chaudhury SK, Mukherjee S, Saha P, Mukherjee U, Das PK, Banerjee R (2011) AC conductivity and dielectric analysis of graphite–clay nanocomposite. Can J Phys 89:1255–1260
22. Wu X, Qi S, Duan G (2012) Polyaniline/graphite nanosheet, polyaniline/Ag/graphite nanosheet, polyaniline/Ni/graphite nanosheet composites and their electromagnetic properties. Synth Met 162(17–18):1609–1614